BMC Biotechnology

RESEARCH

Open Access

Biocompatibility and potential anticancer activity of gadolinium oxide (Gd_2O_3) nanoparticles against nasal squamous cell carcinoma

Xiaopeng Sun[1,2] and Bo Kou[1*]

Abstract

Chemotherapy as a cornerstone of cancer treatment is slowly being edged aside owing to its severe side effects and systemic toxicity. In this case, nanomedicine has emerged as an effective tool to address these drawbacks. Herein, a biocompatible carrier based on bovine serum albumin (BSA) coated gadolinium oxide nanoparticles (Gd_2O_3@BSA) was fabricated for curcumin (CUR) delivery and its physicochemical features along with its potential anticancer activity against nasal squamous cell carcinoma were also investigated. It was found that the fabricated Gd_2O_3@BSA containing CUR (Gd_2O_3@BSA-CUR) had spherical morphology with hydrodynamic size of nearly 26 nm, zeta-potential of -36 mV and high drug (CUR) loading capacity. Drug release profile disclosed that the release of CUR from the prepared Gd_2O_3@BSA-CUR nanoparticles occurred in a sustained- and pH-dependent manner. Also, in vitro cytotoxicity analysis revealed that the fabricated Gd_2O_3@BSA nanoparticles possessed excellent biosafety toward HFF2 normal cells, while Gd_2O_3@BSA-CUR appeared to display the greatest anticancer potential against RPMI 2650 and CNE-1 cancer cell lines. The results also show that the Gd_2O_3@BSA nanoparticles were compatible with the blood cells with minor hemolytic effect (< 3%). The manufactured NPs were found to be completely safe for biological applications in an in vivo subacute toxicity study. Taken together, these finding substantiate the potential anticancer activity of Gd_2O_3@BSA-CUR nanoparticles against nasal squamous cell carcinoma, but the results obtained demand further studies to assess their full potential.

Keywords Gadolinium oxide, Albumin, Curcumin, Nanoparticles, Nasopharyngeal carcinoma, Drug delivery

*Correspondence:
Bo Kou
evankbo@proton.me; evankbo@outlook.com
[1]Department of Otorhinolaryngology head and neck surgery, The First Affiliated Hospital of Xi'an Jiaotong University, Xi'an 710061, Shaanxi, China
[2]Department of Otorhinolaryngology head and neck surgery, The Second Affiliated Hospital of Xi 'an Medical University, Xi'an 710000, Shaanxi, China

Introduction

Cancer as an intricate disease, is the second life threatening disease after cardiovascular disease and accounting for almost 10 million death along with an estimated 19.3 million new cancer cases in 2020 [1]. Nasopharyngeal carcinoma (NPC), as a malignant tumor initiated from head and neck epithelial cell transformation, accounted for 0.7% of global cancer incidents in 2018. Noting 129,000 newly-diagnosed cases of NPC worldwide, mortality rate of female patients were one-third of male patients [2]. The approach to NPC treatment is non-surgical and Chemotherapy is the standard first line systemic approach for treatment of metastatic or recurrent NPC [3]. Chemoradiotherapy has provided NPC patients receiving this conventional therapeutic strategy with a poor quality of life along with causing severe chemotherapy adverse effects such as bone marrow suppression, ototoxicity, neurotoxicity and dysphagia [4–6]. It is urgent to maintain vital functions of five senses while treating the tumor as early as possible which is rarely possible by using conventional modalities such as chemotherapy. In this matter, nanomedicine plays a key role by involving in drug delivery field, reducing necessary dose and ultimately alleviating possible side effects [7, 8]. In virtue of nanomedicine efficacy in NPC treatment, these novel strategies can be used as an alternative to conventional modalities, maximizing therapeutic agent efficacy and penetrating biological barriers [9, 10]. Nanoparticles also have the capability of entrapping poorly-soluble antineoplastic drug, making it possible to be administered intravenously, increasing blood circulation time, altering drug distribution in favor of drug accumulation in tumor site and in some cases overcoming multi-drug resistance [11, 12]. As a category of nanosystems, inorganic nanoparticle can promote optimal drug delivery in terms of bioavailability, biocompatibility, stability and inertness [13, 14]. Another strategy in nanomedicine is utilizing protein nanocarriers for drug delivery due to their special properties such as safety, non-immunogenicity, biodegradability and significant high potential for drug binding [15]. Interestingly, protein nanocarriers can potentially provide targeting features via interacting with specific receptors. Aside from prolonging systemic circulation and enhanced permeation and retention (EPR) effect, albumin protein can induce non-antigenicity in nanoparticles and interact with specific overexpressed receptors in tumors. [16]. To acquire merits of both inorganic and protein nanocarriers and alleviate inorganic nanoparticle pitfalls, inorganic nanoparticles should be coated with proteins, polysaccharides and lipids in which proteins suggest various advantages. It is noteworthy that inorganic nanoparticles can accumulate in body and induce toxicity as a result of high stability [17]. Hybrid-protein inorganic nanoparticles can improve therapeutic efficacy and overcome drug resistance while reducing drug side effect. In this context BSA, has been hybridized with Fe, Au or Gd loaded with different gene or chemotherapeutic agents, previously. Although current standard for advanced NPC involves cisplatin/carboplatin + Gemcitabine/Paclitaxel/5-FU to induce cell apoptosis, overall survival of patients is not satisfactory while presenting intolerable side effects [18, 19]. On the contrary, curcumin (CUR) is well tolerated and exhibit anti-inflammatory and anti-cancer characteristics through pleiotropic properties [20–22]. Because of CUR poor bioavailability and pharmacokinetics, several nanosystems have been designed to facilitate CUR in vivo administration, providing efficient approaches for improving CUR solubility and bioavailability [23, 24]. In the present study we aimed to investigate CUR antineoplastic potential in NPC treatment loaded in Gd_2O_3 inorganic nanoparticles coated with BSA (Gd_2O_3@BSA-CUR). Also, its blood compatibility and cytotoxicity potential against normal cells were investigated in depth.

Materials and methods

Materials

BSA, $Gd(NO_3)_3$, and CUR, were purchased from Sigma-Aldrich (St. Louis, USA). All the other required chemical agents, and solvents that used in this study were of analytical grade and were purchased from Merck (Kenilworth, USA). Materials needed for the in vitro studies were purchased from Gibco.

Methods

Synthesis of BSA coated gadolinium oxide nanoparticles (Gd_2O_3@BSA)

The synthesis of Gd_2O_3@BSA was carried out according to a published procedure with minor modification [25]. In brief, the amount of 0.25 g of BSA was dissolved in distilled water (9 mL), and then 100 mM of gadolinium oxide solution ($Gd(NO_3)_3$, 1.0 mL) was gradually added to the reaction mixture under vigorous stirring. In order to adjust and maintain the pH of the reaction mixture to 12, sodium hydroxide (NaOH) with a concentration of 2.0 M was used. The mixture was then vigorously stirred at room temperature for 12 h to allow the nanocrystal to growth. Finally, the mixture was then dialyzed against distilled water for 48 h to obtain the impurity-free Gd_2O_3@BSA nanoparticles.

Preparation of gadolinium oxide nanoparticles containing CUR

Following the fabrication of Gd_2O_3@BSA nanoparticles, CUR as a natural chemotherapeutic agent was encapsulated to form CUR loaded Gd_2O_3@BSA nanoparticles (Gd_2O_3@BSA-CUR). Briefly, 4 mg of CUR was first dissolved in ethanol and then, slowly added to the

pre-synthesized colloidal dispersion of Gd_2O_3@BSA (10.0 mL, 12 mg) and allowed to be stirred for 24 h, at 37 °C. Finally, the Gd_2O_3@BSA-CUR nanoparticles were collected by centrifuging at 18 000 rpm for 0.5 h, and washing several times with deionized water: ethanol (75: 25) mixture and final wash of water, and suspending them into phosphate-buffer solution. Afterward, to ascertain the amount of drug (CUR) loading, 2 mg of Gd_2O_3@ BSA-CUR nanoparticles were dispersed in ethanol (2 mL) and stirred at room temperature for 24 h with gentle shaking, then the absorbance of the supernatant containing CUR was determined by a UV-vis spectrophotometer at 428 nm.

Release behavior of Gd_2O_3@BSA-CUR

The release behavior of CUR from developed Gd_2O_3@ BSA-CUR nanoparticles was investigated spectrophotometrically by measuring the absorbance of CUR at 428 nm. In this case, dialysis method as a common method of drug release study was carried out under both acidic (pH 4) and neutral (pH 7.2) condition. Accordingly, in a dialysis bag (MWCO 14KDa), 1 mg/mL of Gd_2O_3@BSA-CUR nanoparticles was first dispersed in release/donor medium (PBS: ethanol; 65: 35 v/v) to be dialyzed against 35 mL of acceptor medium outside the dialysis membrane. Subsequently, it was incubated at 37 °C with gentle shaking. CUR release behavior was assessed by taken known amount of aliquots from the acceptor medium outside the dialysis membrane at the predetermined time intervals. Finally, the release of CUR over the time was determined at 428 nm using a UV-Vis spectrophotometer.

Characterization

In order to ensure that whether the Gd_2O_3@BSA nanoparticles were meritoriously synthesized or not, several characterization techniques were used. In this regard, UV-vis spectroscopy analysis were employed to fully characterize the developed Gd_2O_3@BSA nanoparticles structure. UV-vis spectroscopy revealed the possible interaction between the constituents of Gd_2O_3@BSA nanoparticles and confirm the presence of BSA macromolecule along with CUR in the final nanoformulation. To determine the morphology and particle size of fabricated Gd_2O_3@BSA nanoparticles, scanning transmission electron microscopy (STEM, ZEISS), was also applied.

Biuret test

In order to determine the presence of a peptide bond (BSA) in a dispersion containing Gd_2O_3@BSA nanoparticles, biuret test was performed. Typically this assay is based on the color changing through the chemical test called biuret reaction, a violet color is formed once a peptide molecule treated with alkaline copper sulfate (blue color). Therefore to confirm the presence of BSA molecules in the structure of developed Gd_2O_3@BSA nanoparticles, 1–2 mL of PBS and Gd_2O_3@BSA suspension were separately added to a clean and dry test tubes then amount of 1–2 mL of Biuret reagent was introduced to each tube. After 5 min. of incubation at room temperature with gentle shaking the test tubes were monitored for any color change.

Size and zeta potential

It has been reported that, nanosuspension with mean particle size between 1 and 100 nm exhibited higher intracellular uptake, lower hepatic filtration and longer blood circulation half-life in vivo. Accordingly, mean hydrodynamic particle size and zeta potential of Gd_2O_3@ BSA and Gd_2O_3@BSA-CUR nanoparticles were determined using dynamic light scattering (DLS) on a nano/ zetasizer (Malvern Instruments, Worcestershire, UK, ZEN 3600 model Nano ZS).

Hemolysis test

Herein, the hemolytic activity of Gd_2O_3@BSA nanoparticles was carried out according to a previously established protocol [26].

Analysis of cytotoxicity against normal cells

To further insure the biosafety of developed Gd_2O_3@BSA nanoparticles as a biocompatible drug carrier its in vitro potential cytotoxicity toward normal cells (HFF-2 cells) was performed using MTT assay in accordance with a previously stablished protocols [27]. It is anticipated that the prepared Gd_2O_3@BSA nanoparticles would have no cytotoxicity toward HFF-2 cells. Accordingly, HFF-2 cells were seeded in a 96-well plate (1×10^4 cells per well) and incubated for 24 h at 37 °C. After that cells were treated with Gd_2O_3@BSA nanoparticles at different concentration ranging from 32.5 to 520 µg / mL and were incubated for another 24 h to elucidate whether the developed drug vehicles are safe to the normal cells or not. After this step, the previous medium was replaced with as prepared MTT solution (20 µL with concentration of 2.5 mg / mL). Within incubation time of 4 h at 37 °C, the purple insoluble formazan crystals is formed and 100 mL of DMSO was introduced to each well to dissolve the formed formazan dyes. Finally, the optical density (OD) of formazan was read using microplate reader (Bio-Tek, USA) at 570 nm. This analysis was performed in quintuplicate ($n=5$).

In vitro anti-cancer activity

MTT assay was also performed to find out the potential anticancer activity of Gd_2O_3@BSA, Gd_2O_3@BSA-CUR nanoparticles and free CUR against nasal squamous cell carcinoma (RPMI 2650) and human nasopharyngeal

carcinoma epithelioid cell line (CNE-1) according to a previously stablished protocols [27]. Similar procedure as described in the previous section was performed, except that RPMI 2650 and CNE-1 cancer cell lines were used instead of HFF-2 cells. Briefly, cells were seeded in a 96-well plate (1×10^4 cells per well), and after reaching to the desired confluency, cells were then treated and incubated (24 h) with free CUR (serial concentrations 7.5–120 µg / mL) Gd_2O_3@BSA-CUR nanoparticles (7.5–120 µg / mL of CUR) and Gd_2O_3@BSA (equivalent content), to unveil the potential anticancer effects of developed nanoparticles. Medium that received no experimental treatment was considered as control group. After 24 h of incubation of cells with foregoing nanoparticles, the medium was removed and replaced with as prepared MTT solution (20 µL with concentration of 2.5 mg / mL). Within 4 h incubation at 37 °C, the purple insoluble formazan dyes is formed and so 100 mL of DMSO was introduced to each well to dissolve formazan dyes. Finally, the optical density (OD) of formazan which its intensity indicate the cell viability was read using microplate reader (Bio-Tek, USA) at 570 nm. This analysis was performed in quintuplicate ($n=5$). Each concentrations were tested five times in a single run at the same condition.

In vivo Biocompatibility study

BALB/c mice were purchased from Beijing Vital River Laboratory Animal Technology Co., Ltd. Gd_2O_3@BSA was injected into female BALB/c mice ($N=4$) at different dosages (25, 50, and 100 mg kg-1), and the mice's weight and mortality were monitored to determine the in vivo biosafety of the substance. Hematoxylin and eosin (H&E) staining was used to assess effect of NPs on key organs of mice that were given the highest dose. At the end of the study, the animals were euthanized. Mice were placed in the euthanasia chamber, and then introduce 100% CO2 at a flow rate between 30 and 40% of the chamber volume per min.

Statistical analysis

All of the quantitative data were expressed as mean with standard deviation (mean ± SD) unless otherwise stated. Also statistical analysis was performed using GraphPad Prism software (GraphPad Prism 8).

Results and discussion

Characterization

Several techniques have been applied to characterize the as-prepared nanocarrier and Gd_2O_3@BSA-CUR nanoparticles. In terms of size and morphology of the fabricated nanocarrier and Gd_2O_3@BSA-CUR nanoparticles, STEM was performed. As shown in Fig. 1a all of the developed nanoparticles were monodispersed and had spherical morphology with mean diameter smaller than 10 nm. Furthermore, no aggregation was found in the STEM image of developed Gd_2O_3@BSA-CUR.

Biuret test

To confirm the presence of BSA in nanosuspension of Gd_2O_3@BSA nanoparticles, biuret test was carried out. Generally, this assay is based on the color changing in which the blue color of alkaline copper sulfate changed to the violet color. As shown in Fig. 1b, the test tube that contains no experimental test agents have a blue color while the suspension contain Gd_2O_3@BSA nanoparticles react with biuret agents and the color turned to the violet color and underline that the Gd_2O_3 is successfully decorated with BSA macromolecules [28]. These results have strength our confidence in presence of protein (BSA) in the structure of developed nanocarriers.

Size and zeta potential

Nanoparticles for drug delivery vary in size but their size generally lies between 100 and 500 nm [29]. However, nanoparticles with size smaller than 100 nm considered as an optimal size for effective delivery of drugs in biomedical application. Beside this, stability of nanoparticles in biological microenvironment is another major factor which can highly restrict the utilization of nanodrug delivery systems. Zeta potential or surface charge of nanoparticles is an important features in which the value of this parameters considered as an indicator for physical stability. In other words, zeta potential can directly affect the colloidal stability in which the higher the magnitude of zeta potential demonstrate the excellent stability of nanoparticles [30]. Moreover, the initial adsorption of nanoparticles and its interaction with biological components such as cell membrane is strongly dependent on zeta potential [31]. Once the adsorption of nanoparticles occurred, particle size is influential factor in their endocytotic uptake rate. Accordingly, both size and zeta potential of Gd_2O_3@BSA and Gd_2O_3@BSA-CUR nanoparticles were determined. As shown in Fig. 1c, the mean hydrodynamic size of Gd_2O_3@BSA was 17 nm and its corresponding poly dispersity index (PDI) 0.419, while by addition of CUR to the Gd_2O_3@BSA, the particle size increased and found to be 26 nm with corresponding PDI of 0.462. These finding indicated that the fabricated nanoparticles had a mean particle size of below 100 nm. DLS measurement also show that the zeta potential of Gd_2O_3@BSA and Gd_2O_3@BSA-CUR was −32 mV and −36 mV, respectively (Fig. 1d). These significant negative surface charge indicated that these particles tend to strongly repel each other than to aggregate in suspension. More importantly, plasma and blood cells have a negative surface charges, therefore, negatively charged nanoparticles are preferable for blood contacting nanoparticles,

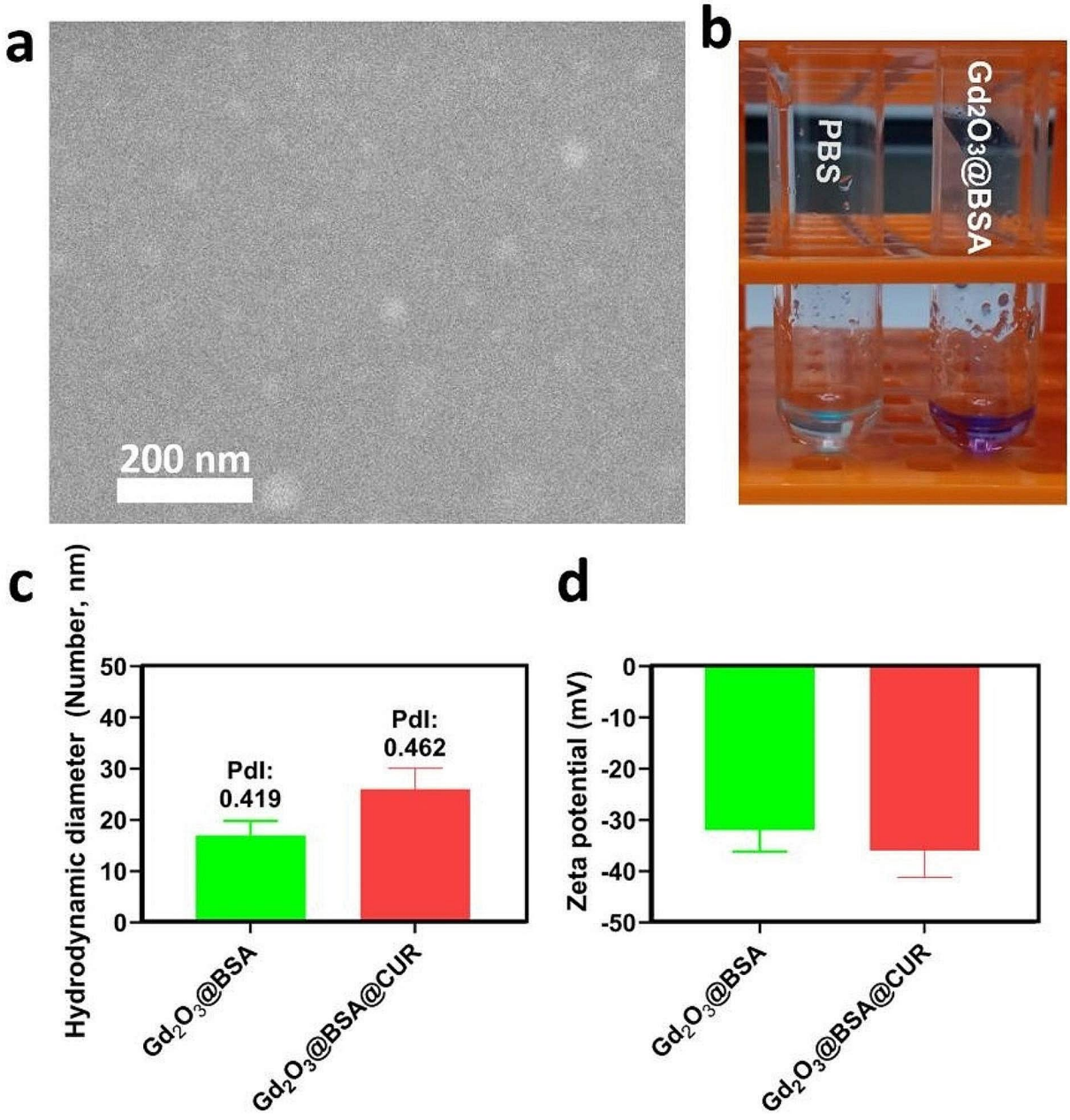

Fig. 1 Morphology, size and zeta potential of developed nanoparticles. (**a**) STEM image of Gd_2O_3@BSA-CUR nanoparticles; (**b**) Biuret test of Gd_2O_3@BSA nanoparticles; (**c**) & (**d**) are size and zeta potential, respectively

as these materials have very low electrostatic interaction with blood components and their blood circulation time is more extended and are more stable than the positively charged nanoparticles. These findings revealed that fabricated nanoparticles were in nano-sized range and possessed excellent physical stability.

UV-Vis analysis

UV-vis spectrophotometer as a facile characterization technique was also applied to study any possible interaction among different components of Gd_2O_3@BSA-CUR nanoparticles. It is also applied to confirm that whether the Gd_2O_3@BSA-CUR nanoparticles were successful synthesized or not. Accordingly, UV−vis spectra of CUR, Gd_2O_3@BSA and Gd_2O_3@BSA-CUR is depicted in Fig. 2a. The obtained UV−vis spectra obviously show

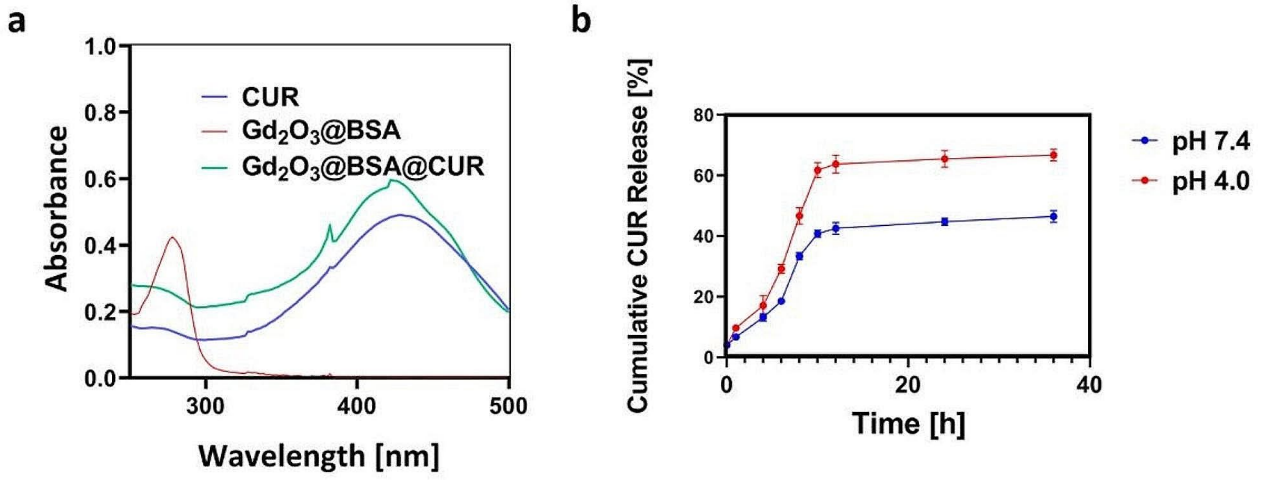

Fig. 2 Characterization and release behavior of Gd_2O_3@BSA-CUR nanoparticles. (**a**) UV-Vis spectra of CUR, Gd_2O_3@BSA and Gd_2O_3@BSA-CUR nanoparticles; and (**b**) drug release profile of Gd_2O_3@BSA-CUR nanoparticles under acidic and normal condition

the presence of Gd_2O_3 nanoparticles in the structure of Gd_2O_3@BSA and Gd_2O_3@BSA-CUR, as its major peak is presented in the spectrum of Gd_2O_3@BSA and Gd_2O_3@BSA-CUR nanoparticles at 265 and 270 nm, respectively [32]. It is worth mention that the characteristic peak of BSA is also assigned at 263 nm which is overlapped with peak of Gd_2O_3 nanoparticles, but as stated previously the Biuret test confirmed the presence of BSA macromolecules. CUR as a natural chemotherapeutic agent was loaded into Gd_2O_3@BSA nanoparticles and its major UV-Vis peak is observed at 430 nm. As shown in Fig. 2a, the vis-UV spectrum of Gd_2O_3@BSA-CUR nanoparticles, in addition to the characteristic peaks of BSA and Gd_2O_3, a broad peak near 400–450 nm can be seen which attributed to the load of CUR and the successful synthesis of final nanotherapeutic is thus approved [33].

Release behavior of Gd_2O_3@BSA-CUR

The release behavior of CUR from the as-prepared Gd_2O_3@BSA-CUR nanoparticles was exploited to determine the release profile of CUR under different condition. UV-Vis analysis showed that drug loading of CUR were found to be 21.3%. Also, it has been well known that pH-sensitive nanoparticles are preferable for delivering chemotherapeutics to acidic microenvironment of tumors since intracellular trafficking of chemotherapeutics in this case increased efficiently and meanwhile systemic toxicity of drugs substantially decreased compared to conventional delivery of drugs via common drug delivery systems [34, 35]. Accordingly, to investigate the tumor microenvironment sensitivity of Gd_2O_3@BSA-CUR nanoparticles, CUR release behavior was assessed under acidic (pH=4) and normal physiological condition (pH=7.4). Drug release profile of CUR from the as-prepared Gd_2O_3@BSA-CUR nanoparticles is displayed in Fig. 2b. pH-dependent release behavior in a sustained/controlled way was observed for CUR. As a matter of fact, acidic pH facilitate the release of CUR compared to normal physiological environment which is favorable in cancer treatment. This release behavior can also alleviate chemotherapy associated side effects, challenges and enhance drug accumulation within tumor tissues rather than normal tissues and theraputics efficacy is thus improved. Figure 2b showed the biphasic release behavior for CUR from Gd_2O_3@BSA-CUR nanoparticles in which the immediate release 43% and 65% within 10 h was observed at pH 7.4 and 4, respectively followed by a plateau behavior up to 40 h. Altogether, pH-dependent release behavior of CUR along with its multiple biological activities makes the designed Gd_2O_3@BSA-CUR nanoparticles as a highly compelling tool for alternative cancer treatment option to chemotherapy.

In vitro biosafety assessment

Hemocompatibility of as-prepared nanovehicle

Chemotherapeutic agents come into critical contact with red blood cells upon drug administration, followed by direct or indirect agent entrance into blood flow. In order to achieve desirable effect, it is mandatory for chemotherapeutic agents and nanoparticles to enter blood flow to be transported to sites of action, tissues and organs. Since direct contact of nanotherapeutic agents with blood components is inevitable, assessment of blood compatibility as a major concern is essential prior to in vivo drug administration. For this purpose hemolytic activity of Gd_2O_3@BSA was evaluated against human red blood cells (HRBCs), one of the restrictions of nanomaterials' application in their clinical translation. Different concentrations of Gd_2O_3@BSA (32.5, 65, 130, 260 and 520 μg/mL), H_2O (positive control, as it

leads to complete hemolysis of HRBCs) and phosphate buffered saline (PBS) (negative control, as it is highly compatible with HRBC) were tested for their hemolytic activity on human RBC. Blood compatibility data of each substance is depicted in Fig. 3a which reveals an increase in hemolytic activity of nanovehicle by increasing vehicle concentration. Nevertheless, hemolytic activity of Gd_2O_3@BSA remained less than 3% even at highest concentration tested (520 µg/mL). These findings are in line with previous studies, investigating G_2O_3-based up-conversion nanoprobes as contrast agents for multi modal imaging [36]. Similarly, Mortezazadeh et al. and his colleague have reported hemolytic activity of Gd_2O_3@PCD-Glu (Gadolinium oxide nanoparticles coated with polycyclodextrin and modified with glucose) less than 5.5% even in concentrations as high as 1 g/mL [37]. Generally, these results offered invaluable evidence for Gd-based nanoparticles' hemocompatibility noting that no severe hemolysis activity was detected. Thus no concern remained regarding safe clinical application of blood-contacting Gd-based nanomaterials.

Cell cytotoxicity

Biosafety of Gd_2O_3@BSA was explored via MTT assay on HFF-2 cell line. Cells were treated with 5 different concentrations of nanovehicle (32.5, 65, 130, 260 and 520 µg/mL). Even in concentrations as high as 520 µg/mL, cells showed good biocompatibility after 24 h of incubation with Gd_2O_3@BSA (Fig. 3b). No significant difference was found between the different concentrations used. Surprisingly, by increasing nanoparticle concentration from 65 to 130 µg/mL and higher, cell growth slightly increased in contrast to control and no growth inhibition was observed. Although cell viability was shown to be slightly lower in 32.5 and 65 µg/mL nanoparticle concentrations than in control conditions, cell viability was close to 100% (Fig. 3b). The surprising results observed under higher nanoparticle concentrations might reflect the fact that nanoparticles act as a cell growth supplement factor due to the presence of albumin, which is consistent with a previous report [38]. Then, Gd_2O_3@BSA can be used safely in the presence of normal cells up to 520 µg/mL and no toxicity is observed.

MTT assay for assessing potential in vitro anticancer properties

The potential anticancer activity of designed NPs was assessed against CNE-1 and RPMI 2650 cells. While it has been shown that several NPC cell lines (e.g. CNE-1, CNE-2, AdAH, NPC-KT, and HONE-1) are contaminated with HeLa cells [39, 40] and thus inadequate to study NPC, we also used RPMI 2650 cells to evaluate the potential anticancer activity of Gd_2O_3@BSA@CUR nanoparticles against nasal squamous cell carcinoma. The results show that NPs show similar anticancer activity against CNE-1 and RPMI 2650 cells (Fig. 3c and d). The data suggest that both CUR and Gd_2O_3@BSA@CUR treatments show significant toxicity on RPMI 2650 cells. Moreover, the nanosystem loaded with CUR, Gd_2O_3@BSA@CUR, exhibited greater cytotoxicity against nasal

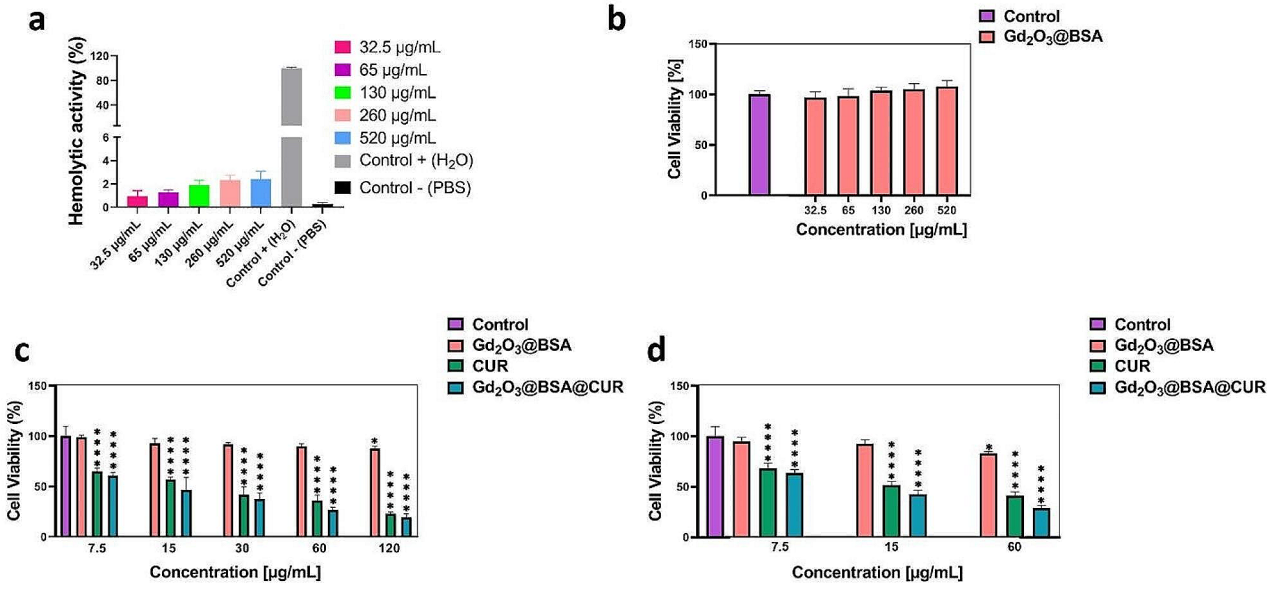

Fig. 3 Biocompatibility, hemocompatibility and cytotoxicity potential of developed nanoparticles. (**a**) hemocompatibility analysis of Gd_2O_3@BSA nanoparticles; (**b**) cytotoxicity potential of Gd_2O_3@BSA nanoparticles against HFF-2, (**c**) Potential anticancer effects of Gd_2O_3@BSA-CUR nanoparticles against CNE-1 cells and (**d**) Potential anticancer effects of Gd_2O_3@BSA-CUR nanoparticles against RPMI 2650 cells

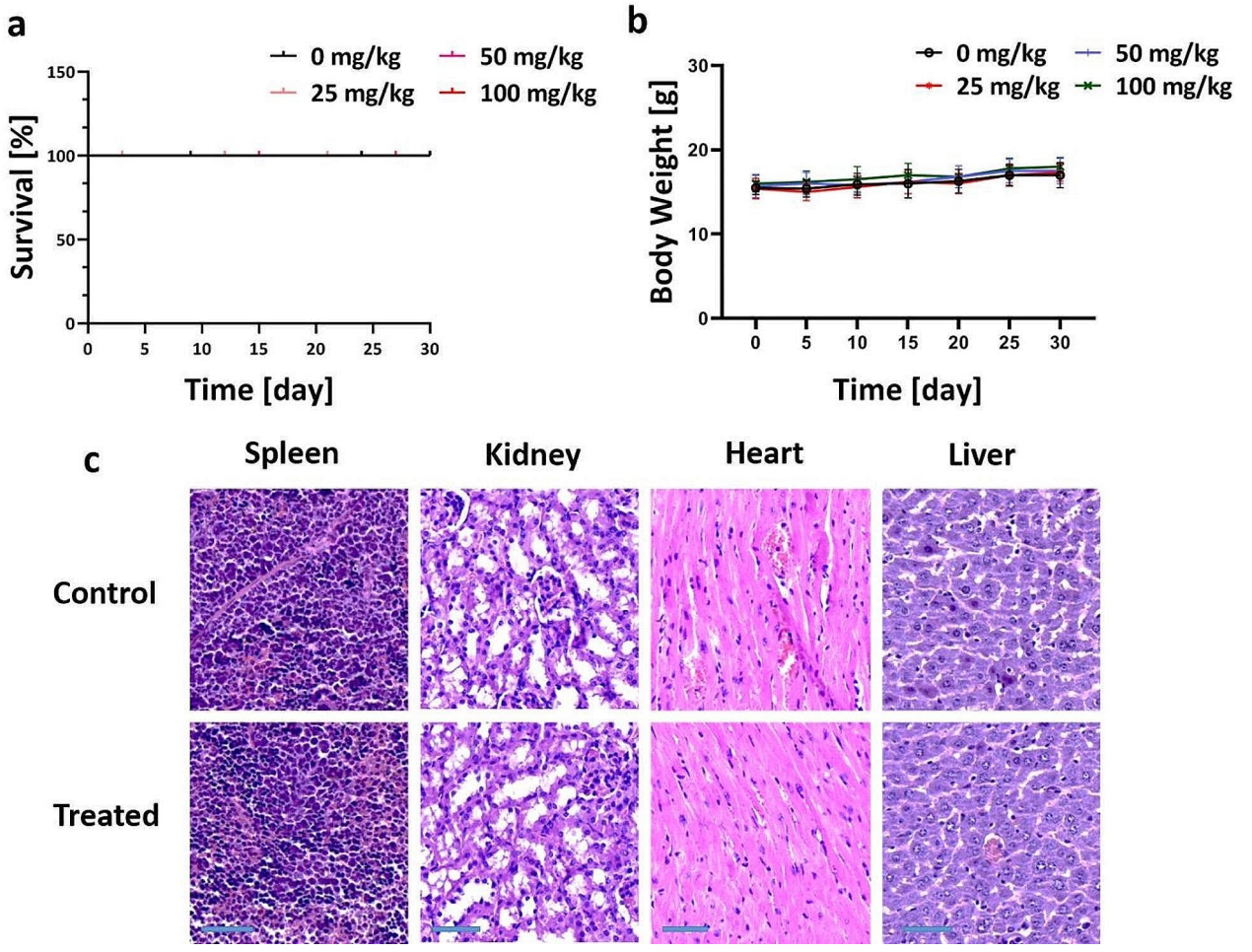

Fig. 4 In vivo biocompatibility studies. (**a**) Cox regression curve of mice injected with Gd_2O_3@BSA NPs. (**b**) Weight of mice injected with Gd_2O_3@BSA NPs. (**c**) Histopathological findings of key organs of mice treated with Gd_2O_3@BSA NPs (scale bar: 50 μm)

squamous cell carcinoma in comparison with CUR condition.

Dose-dependent induction of cell death was evident in both cell lines after treatment with Gd_2O_3@BSA, CUR and Gd_2O_3@BSA@CUR in different concentrations (7.5, 15, 30, 60, 120 μg/mL). As can be seen in Fig. 3c and d, following CUR and Gd_2O_3@BSA@CUR exposure with cells, the cells experienced dose-dependent toxicity. The test revealed that both CUR and Gd_2O_3@BSA@CUR treatments induced significant cell death in CNE-1 and RPMI 2650 cells, where the nanosystem Gd_2O_3@BSA@CUR exhibited a greater toxic effect relative to CUR condition. Unexpectedly for 120 μg/mL value of vehicle concentration, cancerous cell growth inhibition was observed, in comparison with control, while stimulating cell growth in normal cells at 130 μg/mL concentration. We are of the opinion that the vehicle itself has a suppressive effect on cancerous cell growth which shows potential anticancer effect of inert inorganic element, Gd. This finding reinforces usefulness of hybrid-protein nanosystems as drug delivery system for chemotherapeutic agents such as CUR. CUR inhibitory effect on cancerous cell viability is previously determined in case of CNE-2Z, CNE-1 and HONE-1 cell lines by cell apoptosis induction through caspase-3 activation and MAPK signaling inactivation. [41].

CUR's diverse effects on cancer cells are probably attributed to a variety of mechanisms of action. It has been reported that CUR shows both a mitotic and G1/S arrest, then induces apoptosis [42, 43]. Experimental evidence indicates a wide array of molecular targets affected by curcumin, encompassing transcription factors, cell cycle proteins, enzymes, cell surface adhesion proteins, and cytokines [44]. Curcumin has been associated with the inhibition of cell signaling pathways, including those involving Akt, NF-κB, AP-1, or JNK. Additionally, there is evidence of up-regulation of growth arrest and DNA damage-inducible (GADD) genes, along with down-regulation of the expression of survival genes like egr-1, c-myc, bcl-X(L), and IAP. Moreover, abnormalities in

tumor suppressor genes, such as p53, have been implicated [45, 46].

Moreover, gadolinium oxide-modified with polyesters based on ß-cyclodextrine proved to be an efficient system for drug delivery of doxorubicin against 4T1 cell line [47]. Notably, BSA is also used frequently for coating nanoparticles and enhancing biocompatibility of drug delivery systems decorated with biological macromolecules [48, 49]. Altogether, these findings suggest that Gd_2O_3@BSA could be a proper carrier for the delivery of chemotherapeutics and may improve their therapeutic efficacy when as well.

In vivo biocompatibility study

In vivo biosafety was used to make sure that nanoparticles were safe in living organisms and, as a result, to increase their chances of being good candidates for preclinical studies. Mice were given different doses of nanoparticles, and their behavior and survival rate were recorded. As can be seen in Fig. 4a and b at any of the tested injection doses, there were no fatalities and no observable abnormal weight increase or loss compared to the control group, which confirm the biocompatibility of Gd_2O_3@BSA in studied dose. Also histopathological findings show that there were no major alterations or signs of toxicity found in the histopathology of the liver, kidney, spleen, or heart. There was no sign of necrosis or any other abnormalities at studied organs (Fig. 4c). However, it is critical to consider long-term safety and potential cumulative effects, before translating to clinic.

Conclusions

In this study, we developed hybrid nanoparticles based on gadolinium oxide nanoparticles decorated with BSA macromolecules (Gd_2O_3@BSA) for CUR delivery and have demonstrated the feasibility in vitro. It was characterized in terms of chemical structure, morphology, size, zeta potential, toxicity, biocompatibility along with its in vitro cytotoxicity against RPMI 2650 cells. Gd_2O_3@BSA-CUR showed pH-dependent CUR release while maintaining their anticancer property. Notably, Gd_2O_3@BSA-CUR significantly inhibited cell growth and enhanced therapeutic efficacy compared with free CUR. Our study shows the potential of using gadolinium oxide (Gd_2O_3) nanoparticles against nasal squamous cell carcinoma.

Abbreviations

BSA	Bovine serum albumin
BSA	Coated gadolinium oxide nanoparticles Gd2O3@BSA
CUR	Curcumin
CUR	Loaded Gd2O3@BSA nanoparticles Gd2O3@BSA-CUR
NPC	Nasopharyngeal carcinoma
EPR	Enhanced permeation and retention
NaOH	Sodium hydroxide
STEM	Scanning transmission electron microscopy
UV-vis	Ultraviolet–visible spectroscopy
DLS	Dynamic light scattering
MTT	3-(4,5-dimethylthiazol-2-yl)-2,5-diphenyltetrazolium bromide
DMSO	Dimethyl sulfoxide
OD	Optical density
H&E	Hematoxylin and eosin
PDI	Poly dispersity index
HRBCs	Human red blood cells
PBS	Phosphate buffered saline

Acknowledgements

This work was supported by the Second Affiliated Hospital of Xi 'an Medical University.

Author contributions

X. S.: Methodology, Investigation, original draft preparation. B. K.: Methodology, Writing-review & editing.

Funding

No funding was received.

Data availability

The datasets generated and/or analysed during the current study are not publicly available due the data also forms part of an ongoing study but are available from the corresponding author on reasonable request.

Declarations

Ethics approval and consent to participate

Ethics Committee of the Second Affiliated Hospital of Xi 'an Medical University has approved the current study. All methods were carried out in accordance with relevant guidelines and regulations.

Consent to participate

Not applicable.

Consent to publish

Not applicable.

Competing interests

The authors declare no competing interests.

Received: 13 July 2023 / Accepted: 11 July 2024
Published online: 06 August 2024

References

1. Sung H, Ferlay J, Siegel RL, Laversanne M, Soerjomataram I, Jemal A, et al. Global Cancer statistics 2020: GLOBOCAN estimates of incidence and Mortality Worldwide for 36 cancers in 185 countries. CA Cancer J Clin. 2021;71(3):209–49.
2. Bray F, Ferlay J, Soerjomataram I, Siegel RL, Torre LA, Jemal A. Global cancer statistics 2018: GLOBOCAN estimates of incidence and mortality worldwide for 36 cancers in 185 countries. Cancer J Clin. 2018;68(6):394–424.
3. Mai H-Q, Chen Q-Y, Chen D, Hu C, Yang K, Wen J, et al. Toripalimab or placebo plus chemotherapy as first-line treatment in advanced nasopharyngeal carcinoma: a multicenter randomized phase 3 trial. Nat Med. 2021;27(9):1536–43.
4. Rezende TMB, Freire MS, Franco OL. Head and neck cancer: proteomic advances and biomarker achievements. Cancer. 2010;116(21):4914–25.
5. Birkeland AC, Swiecicki PL, Brenner JC, Shuman AG. A review of drugs in development for the personalized treatment of head and neck squamous cell carcinoma. Expert Rev Precision Med drug Dev. 2016;1(4):379–85.
6. Caponigro F, Longo F, Ionna F, Perri F. Treatment approaches to nasopharyngeal carcinoma: a review. Anticancer Drugs. 2010;21(5):471–7.
7. Wei W, Zarghami N, Abasi M, Ertas YN, Pilehvar Y. Implantable magnetic nanofibers with ON–OFF switchable release of curcumin for possible local hyperthermic chemotherapy of melanoma. J Biomedical Mater Res Part A. 2022;110(4):851–60.
8. Talaei S, Mellatyar H, Pilehvar-Soltanahmadi Y, Asadi A, Akbarzadeh A, Zarghami N. 17-Allylamino-17-demethoxygeldanamycin loaded PCL/PEG

nanofibrous scaffold for effective growth inhibition of T47D breast cancer cells. J Drug Deliv Sci Technol. 2019;49:162–8.
9. Xu L, Zhou C, Wang F, Liu H, Dong G, Zhang S, et al. Functional drug carriers formed by RGD-modified β-CD-HPG for the delivery of docetaxel for targeted inhibition of nasopharyngeal carcinoma cells. RSC Adv. 2022;12(28):18004–11.
10. Liu Z, Wang P, Xie F, Chen J, Cai M, Li Y, et al. Virus-inspired Hollow Mesoporous Gadolinium-Bismuth Nanotheranostics for Magnetic Resonance Imaging-guided synergistic photodynamic-Radiotherapy. Adv Healthc Mater. 2022;11(6):2102060.
11. Li Y, Ertas YN, Jafari A, Taheri M, Pilehvar Y. Co-delivery of curcumin and chrysin through pH-sensitive hyaluronan-modified hollow mesoporous silica nanoparticles for enhanced synergistic anticancer efficiency against thyroid cancer cells. J Drug Deliv Sci Technol. 2023;87:104787.
12. Gao Y, Wang R, Huang T, Tian Q, Yang C, Pilehvar Y, et al. Synthesis and characterization of rutin-loaded micelles for glioblastoma multiforme treatment: a computational and experimental study. J Drug Deliv Sci Technol. 2023;86:104675.
13. Serati-Nouri H, Mahmoudnezhad A, Bayrami M, Sanajou D, Tozihi M, Roshangar L, et al. Sustained delivery efficiency of curcumin through ZSM-5 nanozeolites/electrospun nanofibers for counteracting senescence of human adipose-derived stem cells. J Drug Deliv Sci Technol. 2021;66:102902.
14. Ahmadi S, Pilehvar Y, Zarghami N, Abri A. Efficient osteoblastic differentiation of human adipose-derived stem cells on TiO2 nanoparticles and metformin co-embedded electrospun composite nanofibers. J Drug Deliv Sci Technol. 2021;66:102798.
15. Elzoghby AO, Samy WM, Elgindy NA. Protein-based nanocarriers as promising drug and gene delivery systems. J Controlled Release. 2012;161(1):38–49.
16. Elzoghby AO, Hemasa AL, Freag MS. Hybrid protein-inorganic nanoparticles: from tumor-targeted drug delivery to cancer imaging. J Controlled Release. 2016;243:303–22.
17. Kango S, Kalia S, Celli A, Njuguna J, Habibi Y, Kumar R. Surface modification of inorganic nanoparticles for development of organic–inorganic nanocomposites—A review. Prog Polym Sci. 2013;38(8):1232–61.
18. Blagosklonny MV. Prospective strategies to enforce selectively cell death in cancer cells. Oncogene. 2004;23(16):2967–75.
19. Heslop HE. Combining drugs and biologics to treat nasopharyngeal cancer. Mol Ther. 2014;22(1):8–9.
20. He X, Zhang C, Amirsaadat S, Jalil AT, Kadhim MM, Abasi M, et al. Curcumin-loaded mesenchymal stem cell–derived exosomes efficiently attenuate proliferation and inflammatory response in Rheumatoid Arthritis Fibroblast-Like synoviocytes. Appl Biochem Biotechnol. 2023;195(1):51–67.
21. Jiang T, Han Y, Esmaeilizadeh N, Barkhordari A, Jalil AT, Saleh MM et al. Epidural Administration of Curcumin-Loaded Polycaprolactone/Gelatin Electrospun Nanofibers for Extended Analgesia after Laminectomy in rats. Appl Biochem Biotechnol. 2023:1–15.
22. Dadashpour M, Pilehvar-Soltanahmadi Y, Zarghami N, Firouzi-Amandi A, Pourhassan-Moghaddam M, Nouri M. Emerging importance of phytochemicals in regulation of stem cells fate via signaling pathways. Phytother Res. 2017;31(11):1651–68.
23. Montazeri M, Pilehvar-Soltanahmadi Y, Mohaghegh M, Panahi A, Khodi S, Zarghami N, et al. Antiproliferative and apoptotic effect of dendrosomal curcumin nanoformulation in P53 mutant and wide-type cancer cell lines. Anti-cancer Agents Med Chem (Formerly Curr Med chemistry-anti-cancer Agents). 2017;17(5):662–73.
24. Mashayekhi S, Rasoulpoor S, Shabani S, Esmaeilizadeh N, Serati-Nouri H, Sheervalilou R, et al. Curcumin-loaded mesoporous silica nanoparticles/nanofiber composites for supporting long-term proliferation and stemness preservation of adipose-derived stem cells. Int J Pharm. 2020;587:119656.
25. Zhou L, Yang T, Wang J, Wang Q, Lv X, Ke H, et al. Size-tunable Gd2O3@ albumin nanoparticles conjugating chlorin e6 for magnetic resonance imaging-guided photo-induced therapy. Theranostics. 2017;7(3):764.
26. Rashidzadeh H, Rezaei SJT, Zamani S, Sarijloo E, Ramazani A. pH-sensitive curcumin conjugated micelles for tumor triggered drug delivery. J Biomater Sci Polym Ed. 2021;32(3):320–36.
27. Rezaei SJT, Sarijloo E, Rashidzadeh H, Zamani S, Ramazani A, Hesami A, et al. pH-triggered prodrug micelles for cisplatin delivery: preparation and in vitro/vivo evaluation. Reactive Funct Polym. 2020;146:104399.
28. Jain A, Jain R, Jain S. Quantitative Analysis of Proteins by various methods including Biuret. Basic techniques in Biochemistry, Microbiology and Molecular Biology. Springer; 2020. pp. 185–9.
29. Rizvi SA, Saleh AM. Applications of nanoparticle systems in drug delivery technology. Saudi Pharm J. 2018;26(1):64–70.
30. Honary S, Zahir F. Effect of Zeta potential on the properties of nano-drug delivery systems-a review (part 2). Trop J Pharm Res. 2013;12(2):265–73.
31. Schwegmann H, Feitz AJ, Frimmel FH. Influence of the Zeta potential on the sorption and toxicity of iron oxide nanoparticles on S. Cerevisiae and E. Coli. J Colloid Interface Sci. 2010;347(1):43–8.
32. Jeon S, Ko J-W, Ko W-B. Synthesis of Gd2O3 nanoparticles and their photocatalytic activity for degradation of azo dyes. Catalysts. 2021;11(6):742.
33. Nosrati H, Baghdadchi Y, Abbasi R, Barsbay M, Ghaffarlou M, Abhari F, et al. Iron oxide and gold bimetallic radiosensitizers for synchronous tumor chemoradiation therapy in 4T1 breast cancer murine model. J Mater Chem B. 2021;9(22):4510–22.
34. Jing X, Hu H, Sun Y, Yu B, Cong H, Shen Y. The intracellular and extracellular microenvironment of Tumor Site: the trigger of Stimuli-Responsive Drug Delivery systems. Small Methods. 2022:2101437.
35. Xu Z, Yang D, Long T, Yuan L, Qiu S, Li D, et al. pH-Sensitive nanoparticles based on amphiphilic imidazole/cholesterol modified hydroxyethyl starch for tumor chemotherapy. Carbohydr Polym. 2022;277:118827.
36. Liu Z, Pu F, Huang S, Yuan Q, Ren J, Qu X. Long-circulating Gd2O3:Yb3+, Er3 + up-conversion nanoprobes as high-performance contrast agents for multi-modality imaging. Biomaterials. 2013;34(6):1712–21.
37. E TM, N G, A EM RASH. Glucosamine conjugated Gadolinium (III) Oxide nanoparticles as a Novel targeted contrast Agent for Cancer diagnosis in MRI. J Biomedical Phys Eng. 2020;10(1):25–38.
38. Pardhiya S, Priyadarshini E, Rajamani P. In vitro antioxidant activity of synthesized BSA conjugated manganese dioxide nanoparticles. SN Appl Sci. 2020;2(9):1597.
39. Chan SY-Y, Choy K-W, Tsao S-W, Tao Q, Tang T, Chung GT-Y, et al. Authentication of nasopharyngeal carcinoma tumor lines. Int J Cancer. 2008;122(9):2169–71.
40. Strong MJ, Baddoo M, Nanbo A, Xu M, Puetter A, Lin Z. Comprehensive high-throughput RNA sequencing analysis reveals contamination of multiple nasopharyngeal carcinoma cell lines with HeLa cell genomes. J Virol. 2014;88(18):10696–704.
41. Momtazi-Borojeni AA, Ghasemi F, Hesari A, Majeed M, Caraglia M, Sahebkar A. Anti-cancer and radio-sensitizing effects of curcumin in nasopharyngeal carcinoma. Curr Pharm Design. 2018;24(19):2121–8.
42. Sa G, Das T. Anti cancer effects of curcumin: cycle of life and death. Cell Div. 2008;3:1–14.
43. Shishodia S, Amin HM, Lai R, Aggarwal BB. Curcumin (diferuloylmethane) inhibits constitutive NF-κB activation, induces G1/S arrest, suppresses proliferation, and induces apoptosis in mantle cell lymphoma. Biochem Pharmacol. 2005;70(5):700–13.
44. Sharma R, Gescher A, Steward W. Curcumin: the story so far. Eur J Cancer. 2005;41(13):1955–68.
45. Sharma RA, Gescher AJ, Steward WP. Curcumin: the story so far. Eur J Cancer. 2005;41(13):1955–68.
46. Han S-S, Chung S-T, Robertson DA, Ranjan D, Bondada S. Curcumin causes the growth arrest and apoptosis of B cell lymphoma by downregulation of egr-1, c-myc, bcl-XL, NF-κB, and p53. Clin Immunol. 1999;93(2):152–61.
47. Mortezazadeh T, Gholibegloo E, Khoobi M, Alam NR, Haghgoo S, Mesbahi A. In vitro and in vivo characteristics of doxorubicin-loaded cyclodextrine-based polyester modified gadolinium oxide nanoparticles: a versatile targeted theranostic system for tumour chemotherapy and molecular resonance imaging. J Drug Target. 2020;28(5):533–46.
48. He J, Feng M, Zhou X, Ma S, Jiang Y, Wang Y, et al. Stabilization and encapsulation of recombinant human erythropoietin into PLGA microspheres using human serum albumin as a stabilizer. Int J Pharm. 2011;416(1):69–76.
49. Chen Q, Wang C, Cheng L, He W, Cheng Z, Liu Z. Protein modified upconversion nanoparticles for imaging-guided combined photothermal and photodynamic therapy. Biomaterials. 2014;35(9):2915–23.

Publisher's Note